

Optimized Schwarz Methods and model adaptivity in electrocardiology simulations

Luca Gerardo-Giorda, Lucia Mirabella, Mauro Perego and Alessandro Veneziani

Abstract The *Bidomain* model is nowadays one of the most accurate mathematical descriptions of the action potential propagation in the heart. However, its numerical approximation is in general fairly expensive as a consequence of the mathematical features of this system, and several works have been devoted to devise effective solvers and preconditioners, [15, 11] among others. A simplification of this model, called *Monodomain* problem is often adopted in order to reduce computational costs of the numerical solution of the cardiac potential. The latter model is however less accurate. A possible trade-off between accuracy and cost is a *model adaptive strategy*. The computational domain is subdivided into regions, coupled through an Optimized Schwarz Method, in which either the Bidomain or the Monodomain problem is solved, according to an *a-posteriori* model error estimator following the spatio-temporal evolution of the action potential propagation. Here we present a possible implementation of this approach, following up previous works on the error estimation and the Optimized Schwarz coupling.

1 Numerical Models for the Cardiac Potential

At the macroscopic level, the myocardial tissue can be regarded as the superposition of two continuous and anisotropic media, the intra-cellular and the extra-cellular

Luca Gerardo-Giorda
BCAM - Basque Center for Applied Mathematics, Bilbao, Spain, e-mail: lgerardo@bcamath.org

Lucia Mirabella
“W.H. Coulter” Dept. Biomed. Engrg., GaTech, Atlanta, GA, USA, e-mail: lucia.mirabella@bme.gatech.edu

Mauro Perego
Dept. of Sci. Comp., Florida State University, Tallahassee, FL, USA, e-mail: mperego@fsu.edu

Alessandro Veneziani
Dept. of Math. and CS, Emory University, Atlanta, GA, USA, e-mail: ale@mathcs.emory.edu

one. They coexist and are connected by a cell membrane, whose capacitance is denoted by C_m . The tissue conductivity depends upon its cells orientation, and in the most general case the associated tensor is anisotropic [7, 14]. In any point $x \in \Omega$, where Ω is the spatial domain under consideration, it is possible to identify an orthonormal triplet of directions, $a_l(x)$, $a_i(x)$, $a_n(x)$, with $a_l(x)$ parallel to the fibers direction, and we denote by σ_τ^l , σ_τ^i , and σ_τ^n ($\tau = i, e$) the corresponding intra and extracellular conductivity coefficients. The conductivity tensors are given by

$$\mathbf{D}_\tau(x) = \sigma_\tau^l(x)a_l(x)a_l^T(x) + \sigma_\tau^i(x)a_i(x)a_i^T(x) + \sigma_\tau^n(x)a_n(x)a_n^T(x), \quad \tau = i, e. \quad (1)$$

We assume that \mathbf{D}_τ fulfill in Ω a uniform elliptic condition.

The Bidomain model. The Bidomain model is a nonlinear reaction-diffusion system of parabolic type describing the spatio-temporal dynamics of the *intra* and *extracellular* potentials, denoted by u_i and u_e , while the cell membrane is regarded as dislocated in the domain [2]. We rely in this paper on a non-symmetric formulation in terms of the transmembrane potential $u = u_i - u_e$, and the extracellular one [4]. We denote by $\mathbf{u} = (u, u_e)^T$ the unknown, by $V = H^1(\Omega) \setminus \{c : c \in \mathbb{R}\}$ and by letting

$$\mathbf{D} = \begin{bmatrix} \frac{\sigma_e^l \mathbf{D}_i}{\sigma_i^l + \sigma_e^l} & \frac{\sigma_e^l \mathbf{D}_i - \sigma_i^l \mathbf{D}_e}{\sigma_i^l + \sigma_e^l} \\ \mathbf{D}_i & \mathbf{D}_i + \mathbf{D}_e \end{bmatrix} \quad \mathbf{E}_1 = \begin{bmatrix} 1 & 0 \\ 0 & 0 \end{bmatrix} \quad \mathbf{e}_1 = \begin{bmatrix} 1 \\ 0 \end{bmatrix}$$

the Bidomain system reads as follows. Find $\mathbf{u} \in L^2(0, T; H^1(\Omega) \times V)$, such that

$$\chi C_m \mathbf{E}_1 \frac{\partial \mathbf{u}}{\partial t} - \nabla \cdot \mathbf{D} \nabla \mathbf{u} + \chi I_{ion}(u) \mathbf{e}_1 = \mathbf{I}^{app}, \quad (2)$$

where χ is the membrane area per tissue volume ratio, $I_{ion}(u)$ is a nonlinear function of the transmembrane potential u , specified by a ionic model, and where \mathbf{I}^{app} represent the applied current stimuli. Several ionic models are available in literature, from more phenomenological to more accurate ones, but the choice of the nonlinear term $I_{ion}(u)$ does not have any influence on the procedure highlighted in what follows. The problem is completed by suitable initial conditions, and by homogeneous Neumann boundary conditions on $\partial\Omega$, modeling an insulated myocardium. The transmembrane potential u is uniquely determined from (2), while the extracellular potential u_e is determined up to a function of time, and is usually identified by imposing a zero average at each time ($\int_\Omega u_e(x, t) dx = 0$, for all $t \in (0, T)$).

The Monodomain model. The Monodomain model is a simplified model for the propagation of the electrical stimulus, based upon a proportionality assumption between the intracellular and the extracellular conductivity tensors, namely assuming $\mathbf{D}_e = \lambda \mathbf{D}_i$, where λ is a constant to be properly chosen. We assume here $\lambda = \sigma_e^l / \sigma_i^l$ [6], and the Monodomain model reads as follows. Find $u \in L^2(0, T; H^1(\Omega))$, such that

$$\chi C_m \frac{\partial u}{\partial t} - \nabla \cdot \frac{\sigma_e^l \mathbf{D}_i}{\sigma_i^l + \sigma_e^l} \nabla u + \chi I_{ion}(u) = I^{app}. \quad (3)$$

Also system (3) is coupled with suitable initial conditions, and homogeneous Neumann boundary conditions on $\partial\Omega$. Differently from the Bidomain, the Monodomain model features a unique solution and is cheaper to solve numerically. In absence of applied currents, the Monodomain model is accurate enough to catch the desired dynamics and effects of the action potential propagation [12]. However, the Bidomain model becomes necessary when current stimuli are applied in the extracellular space. Also, the Monodomain is inadequate to simulate defibrillation [16].

1.1 Numerical approximation

Time integration. For simplicity in presentation, we consider a fixed time step Δt , and we denote with superscript n the unknowns computed at time $t^n = n\Delta t$. Both the Bidomain (2) and the Monodomain equations (3) are advanced in $(0, T)$ by a semi-implicit scheme, where the nonlinear term (the ionic current) is evaluated at the previous time step [2, 4]. More precisely, moving from t^n to t^{n+1} we solve in Ω

$$\chi C_m \mathbf{E}_1 \frac{\mathbf{u}^{n+1} - \mathbf{u}^n}{\Delta t} - \nabla \cdot \mathbf{D} \nabla \mathbf{u}^{n+1} = \mathbf{I}^{app} - \chi I_{ion}(u^n) \mathbf{e}_1 \quad (4)$$

for the Bidomain system, and

$$\chi C_m \frac{u^{n+1} - u^n}{\Delta t} - \nabla \cdot \frac{\sigma_e^l \mathbf{D}_i}{\sigma_i^l + \sigma_e^l} \nabla u^{n+1} = \mathbf{I}^{app} - \chi I_{ion}(u^n) \quad (5)$$

for the Monodomain one.

Space discretization. Both Bidomain (4) and Monodomain (5) models are discretized in space by finite elements [2, 8, 15]. When solving the Bidomain system, the unknowns of the fully discrete problem are represented by the vector $(u_h, u_{e,h})^T$, storing the nodal values of the transmembrane and extracellular potentials. The matrix associated with the discrete Bidomain models is given by

$$\mathbf{B} = \begin{bmatrix} \mathbf{B}_{uu} & \mathbf{B}_{ue} \\ \mathbf{B}_{eu} & \mathbf{B}_{ee} \end{bmatrix} = \begin{bmatrix} \frac{\chi C_m}{\Delta t} \mathbf{M} + \frac{\sigma_e^l}{\sigma_i^l + \sigma_e^l} \mathbf{K}_i & \frac{\sigma_e^l}{\sigma_i^l + \sigma_e^l} \mathbf{K}_i - \frac{\sigma_i^l}{\sigma_i^l + \sigma_e^l} \mathbf{K}_e \\ \mathbf{K}_i & \mathbf{K}_i + \mathbf{K}_e \end{bmatrix}, \quad (6)$$

where \mathbf{M} is the mass matrix while \mathbf{K}_i and \mathbf{K}_e are the stiffness matrices associated with the chosen finite elements space.

When solving the Monodomain system, the unknown of the fully discrete problem is u_h , and the associated matrix is simply block \mathbf{B}_{uu} of the matrix \mathbf{B} in (6).

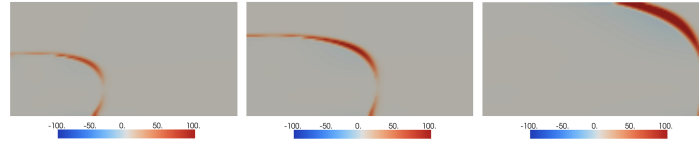


Fig. 1 Differences in the propagation of the membrane potential between Bidomain (u_{Bido}) and Monodomain (u_{Mono}) simulation: $u_{Bido} - u_{Mono}$, with fibers oriented along the x axis (from [6]).

2 A model adaptive strategy

In Fig. 1 (from [6]) we report the differences of the transmembrane potential computed with the Bi- and Monodomain models respectively at different instants. The Figure pinpoints that the differences are mainly concentrated around the wavefront. From these results, we argue that the Monodomain provides an accurate approximation of the potential in most of the region of interest. The *model adaptive strategy* consists then in solving the Bidomain only when actually needed. In a first implementation of this approach [9] a suitable *a posteriori* model estimator was introduced. A hybrid model called *Hybridomain* was advocated. The latter assembles the block \mathbf{B}_{ue} only in correspondence with the nodes identified as Bidomain ones by the model estimator, while the second equation stays untouched. This simplifies significantly the implementation, however the computational advantage is limited, since also in the Monodomain regions an extended problem with the same size of the Bidomain one is solved. An alternative procedure consists of a genuine heterogeneous coupling by splitting the domains where the two models are solved. This coupling raises non trivial issues when matching the two models, featuring a different size. This has been considered in [6], where the Optimized Schwarz method has been advocated for the heterogeneous coupling, addressing the matching conditions at the interface between two different domains. Here, we focus on practical issues when using this approach in realistic problems. A first idea would be to trivially use the *a posteriori* error estimator for detecting the regions where to solve the Bidomain problem and then to couple these subdomains with the Monodomain regions. However, this approach is barely doable. As a matter of fact, the Robin-type interface conditions in the Optimized Schwarz setting require the assembly of mass matrices on the interfaces. As a consequence, every time the Bidomain region changes, one should identify the new interfaces and then recompute the matrices, with an additional computational cost that is anticipated to reduce the advantage of the Optimized Schwarz coupling. The model adaptive strategy we propose here relies instead on a *a priori* subdivision of Ω into smaller subdomains Ω_j . The model error estimator will associate runtime each subdomain with either the Bidomain or the Monodomain problem. In this way, the interfaces matrices needed for the coupling can be computed once at the beginning of the time loop. Notice that the non-symmetric formulation of the Bidomain system ensures that the matrices for the Monodomain model are available after assembling the Bidomain ones.

2.1 Coupling conditions and Optimized Schwarz Methods

We outline here the coupling conditions for the three different types of interfaces. If the subdomains involved have the same characteristic (Bido/Bido and Mono/Mono) the corresponding solutions are labeled by subscript 1 and 2, while if the subdomains have different characteristics (Bido/Mono) the corresponding solutions are labeled with subscript B and M .

Bidomain/Bidomain interface. The coupling conditions on the Bidomain/Bidomain interface have been introduced in [5], and are given by

$$\begin{aligned} \mathbf{n}_1^T \mathbf{D} \nabla \mathbf{u}_1 + \alpha_1 \Sigma \mathbf{u}_1 &= \mathbf{n}_1^T \mathbf{D} \nabla \mathbf{u}_2 + \alpha_1 \Sigma \mathbf{u}_2 \\ \mathbf{n}_2^T \mathbf{D} \nabla \mathbf{u}_2 + \alpha_2 \Sigma \mathbf{u}_2 &= \mathbf{n}_2^T \mathbf{D} \nabla \mathbf{u}_1 + \alpha_2 \Sigma \mathbf{u}_1, \quad \text{where} \quad \Sigma = \begin{bmatrix} \frac{\sigma_e^l}{\sigma_i^l + \sigma_e^l} & 0 \\ 1 & \frac{\sigma_i^l + \sigma_e^l}{\sigma_i^l} \end{bmatrix}. \end{aligned} \quad (7)$$

The convergence of the Optimized Schwarz Algorithm based on the interface conditions (7) was analyzed in [5], where also optimal parameters have been identified by means of Fourier analysis.

Bidomain/Monodomain interface. Due to a dimensional mismatch between the two models, two interface conditions are needed on the Bidomain side of the interface, and one on the Monodomain side [6]. Possible coupling conditions are

$$\begin{aligned} \mathbf{n}_B^T \frac{\sigma_e^l \mathbf{D}_i}{\sigma_i^l + \sigma_e^l} (\nabla u_B + \nabla u_{e,B}) - \mathbf{n}_B^T \frac{\sigma_i^l \mathbf{D}_e}{\sigma_i^l + \sigma_e^l} \nabla u_{e,B} + \frac{\sigma_e^l \alpha}{\sigma_i^l + \sigma_e^l} u_B &= \mathbf{n}_B^T \frac{\sigma_e^l \mathbf{D}_i}{\sigma_i^l + \sigma_e^l} \nabla u_M + \frac{\sigma_e^l \alpha}{\sigma_i^l + \sigma_e^l} u_B \\ \mathbf{n}_B^T \mathbf{D}_i (\nabla u_B + \nabla u_{e,B}) + \mathbf{n}_B^T \mathbf{D}_e \nabla u_{e,B} + \alpha u_B + \frac{\sigma_i^l + \sigma_e^l}{\sigma_i^l} \alpha u_{e,B} &= \alpha u^{rest} \end{aligned} \quad (8)$$

for the Bidomain subproblem, and

$$\mathbf{n}_M^T \frac{\sigma_e^l \mathbf{D}_i}{\sigma_i^l + \sigma_e^l} \nabla u_M + \frac{\sigma_e^l \alpha}{\sigma_i^l + \sigma_e^l} u_M = \mathbf{n}_M^T \frac{\sigma_e^l \mathbf{D}_i}{\sigma_i^l + \sigma_e^l} (\nabla u_B + \nabla u_{e,B}) - \mathbf{n}_M^T \frac{\sigma_i^l \mathbf{D}_e}{\sigma_i^l + \sigma_e^l} \nabla u_{e,B} + \frac{\sigma_e^l \alpha}{\sigma_i^l + \sigma_e^l} u_B \quad (9)$$

for the Monodomain one. To cope with the mismatch, the second condition in (8) is a transparent boundary condition, designed to avoid spurious reflexions off the interface for the extracellular potential wave. The convergence of the Optimized Schwarz Algorithm based on the interface conditions (8)-(9) was analyzed in [6], where also optimal parameters has been identified by means of Fourier analysis.

Monodomain/Monodomain interface. The Optimized Schwarz coupling is significantly simpler on the interface between two Monodomain regions. The semi-implicit temporal integration scheme reduces the problem at each time step to a linear steady reaction-diffusion problem, whose solution by means of Optimized Schwarz Methods has been widely studied, and an optimal parameter has been iden-

tified [3]. The coupling on the interface is given by

$$\begin{aligned} \mathbf{n}_1^T \frac{\sigma_e^l \mathbf{D}_i}{\sigma_i^l + \sigma_e^l} \nabla u_1 + \alpha^{opt} u_1 &= \mathbf{n}_1^T \frac{\sigma_e^l \mathbf{D}_i}{\sigma_i^l + \sigma_e^l} \nabla u_2^p + \alpha^{opt} u_2^p \\ \mathbf{n}_2^T \frac{\sigma_e^l \mathbf{D}_i}{\sigma_i^l + \sigma_e^l} \nabla u_2 + \alpha^{opt} u_2 &= \mathbf{n}_2^T \frac{\sigma_e^l \mathbf{D}_i}{\sigma_i^l + \sigma_e^l} \nabla u_1 + \alpha^{opt} u_1. \end{aligned} \quad (10)$$

2.2 The model error estimator

The *a posteriori* error estimator for choosing between a Bidomain or Monodomain simulation in each subdomain introduced in [9] is based on the extracellular potential computed from a suitable extension of the Monodomain model. More precisely, we let $\mathbf{D}_\varepsilon = \mathbf{D}_e - \frac{\sigma_e^l}{\sigma_i^l} \mathbf{D}_i$. The model estimator is computed at the subdomain level as

$$\zeta_j^2 = \int_{\Omega_j} \nabla u_M \frac{\sigma_i^l \mathbf{D}_\varepsilon}{\sigma_i^l + \sigma_e^l} (\mathbf{D}_i^{-1} + \mathbf{D}_e^{-1}) \frac{\sigma_i^l \mathbf{D}_\varepsilon}{\sigma_i^l + \sigma_e^l} \nabla u_M dx. \quad (11)$$

The value ζ_j^2 is an upper bound for the error in Ω_j between the two models in a $H^1(\Omega_j)$ -type seminorm depending on \mathbf{D}_i and \mathbf{D}_e . The Bidomain model is then activated in Ω_j whenever ζ_j^2 exceeds a given threshold τ_j , depending on the size of the subdomain. Computing ζ_j^2 requires one matrix-vector and one scalar product, and we denote by \mathbf{K}_ε the stiffness matrix associated with (11). More details on this estimator, that we do not report for the sake of space, can be found in [9].

2.3 The model adaptive algorithm

Preprocessing

1. Split the computational domain into non-overlapping subregions Ω_j ($j = 1, \dots, N$).
2. Identify the interfaces Γ_j between subdomains Ω_i and Ω_j .
3. Assemble the local matrices \mathbf{B}_{uu}^j , \mathbf{B}_{ue}^j , \mathbf{B}_{eu}^j , \mathbf{B}_{ee}^j , and \mathbf{K}_ε^j .
4. Assemble the interface mass matrices \mathbf{M}_{Γ_j} .
5. Compute the incomplete ILU factorization of the local \mathbf{B}_{uu}^j and \mathbf{B}_{ee}^j matrices.

Runtime (time step $t^n \rightarrow t^{n+1}$)

1. Run a Monodomain simulation at time t^{n+1} over the whole domain Ω .
2. Evaluate the model estimator and compute the local indicator $\zeta_j^2 = (u_M^j)^T \mathbf{K}_\varepsilon^j u_M^j$.
3. For all Ω_j ($j = 1, \dots, N$) such that $\zeta_j^2 > \tau_j$, activate Bidomain.
4. Run the Optimized Schwarz Algorithm using the solution computed in Step 1 as initial guess. A few iterations are usually enough.

5. Advance to time t^{n+1} .

3 Preliminary numerical results

Numerical results in this section have the purpose to show the effectiveness of the model adaptive method: for this reason we consider here only 2D simulations. The numerical tests are run in Matlab[®] 7.5. The Bidomain problems are solved by a flexible GMRES (f-GMRES) right preconditioned by the Block-triangular preconditioner introduced in [4], while the Monodomain problems are solved by a CG preconditioned by an ILU factorization.

We consider the strip $\Omega = [0, 3] \times [0, 1]$ subdivided into the three nonoverlapping subdomains $\Omega_i = [i - 1, i] \times [0, 1]$, $i = 1, 2, 3$. The fibers are oriented with the principal direction perpendicular to the interfaces, and we impose a stimulus on the whole left boundary of Ω_1 . The well known Rogers-McCulloch ionic model [13] is used.

We plot in Figure 2 the wavefront position at different times (top row), and the activated subdomains (bottom row) during depolarization. The advantage of the model adaptive approach resides in solving only cheap Monodomain problems for the large majority of time steps (in a genuine Monodomain setting, without extensions that were needed by the Hybridomain approach). In Table 1 we report the relative CPU gain over a whole heartbeat duration (450ms) for the model adaptive strategy with respect to the Optimized Schwarz algorithm introduced in [5].

	u_{OSB}	u_{MA}
CPU Time	1.000	0.37

Table 1 Relative CPU time: u_{OSB} and u_{MA} computed with 2 Schwarz iterations.

A more detailed presentation of the method will be the subject of a forthcoming work. Further work needs to be done to identify the proper trade-off between the number of subdomains, and the size of the Bidomain region surrounding the wavefront, and to properly handle the processors load balance in a parallel architecture. Also, dynamical allocation of tasks is under investigation to properly balance, in real problems, the load of each processor in the parallel solver.

References

1. R. H. Clayton, O. M. Bernus, E. M. Cherry, H. Dierckx, F. H. Fenton, L. Mirabella, A. V. Panfilov, F. B. Sachse, G. Seemann, H. Zhang, Models of cardiac tissue electrophysiology: Progress, challenges and open questions, *Progress in biophysics and molecular biology* 104, pp. 22-48, 2011.

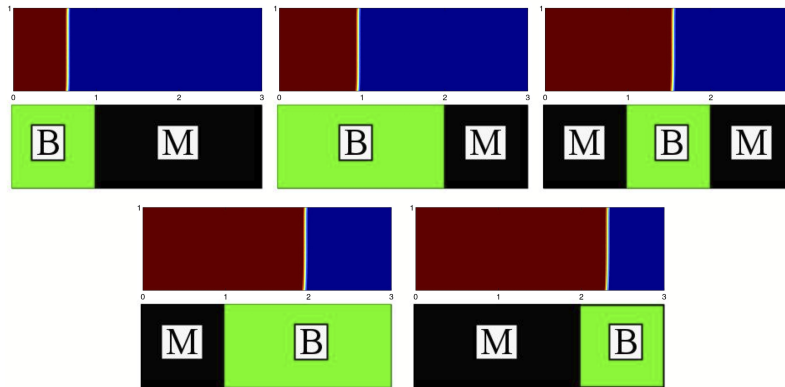


Fig. 2 Propagation of the membrane potential (in red the excited region, top row), and the activated Bidomain region (in green and marked by “B”, bottom row).

2. P. Colli Franzone, L. Pavarino, G. Savaré. Computational electrocardiology: mathematical and numerical modeling, in *Complex Systems in Biomedicine* - A. Quarteroni, L. Formaggia, and A. Veneziani, editors. Springer, Milan, 2006.
3. M.J. Gander. Optimized Schwarz methods. *SIAM J. Num. Anal.*, 44(2), pp. 699–731, 2006.
4. L. Gerardo-Giorda, L. Mirabella, F. Nobile, M. Perego, and A. Veneziani. A model-based block-triangular preconditioner for the Bidomain system in electrocardiology. *J. Comp. Phys.*, 228, pp. 3625–3639, 2009.
5. L. Gerardo-Giorda and M. Perego, Optimized Schwarz Methods for the Bidomain system in electrocardiology *M2AN*, Vol. 47 (2), pp 583–608, 2013.
6. L. Gerardo-Giorda, M. Perego, and A. Veneziani. Optimized Schwarz coupling of Bidomain and Monodomain models in electrocardiology. *M2AN*, Vol. 45 (2), pp. 309–334, 2011.
7. J. Le Grice, B.H. Smaill, and P.J. Hunter. Laminar structure of the heart: a mathematical model. *Am. J. Physiol.*, 272 (Heart Circ. Physiol.)(41):H2466–H2476, 1995.
8. G.T. Lines, M.L. Buist, P. Grottum, A.J. Pullan, J. Sundnes, and A. Tveito. Mathematical models and numerical methods for the forward problem in cardiac electrophysiology *Comput. Visual. Sci.*,5:215–239, 2003.
9. L. Mirabella, F. Nobile, and A. Veneziani. An a posteriori error estimator for model adaptivity in electrocardiology. *Comp. Meth. Appl. Mech. Engrg.*, Vol 200 (37–40), pp. 2727–2737, 2011.
10. L. F. Pavarino and S. Scacchi. Multilevel additive Schwarz preconditioners for the Bidomain reaction-diffusion system. *SIAM J. Sci. Comp.*, 31(1):420–443, 2008.
11. M. Pennacchio and V. Simoncini. Algebraic multigrid preconditioners for the bidomain reaction-diffusion system. *Appl. Num. Math.*, 59(12):3033–3050, 2009.
12. M. Potse, B. Dubé, J. Richer, and A. Vinet. A comparison of Monodomain and Bidomain Reaction-Diffusion models for Action Potential Propagation in the Human Heart. *IEEE Trans. Biomed. Eng.*, 53(12):2425–2435, 2006.
13. J. Rogers and A. McCulloch. A collocation-Galerkin finite element model of cardiac action potential propagation. *IEEE Transactions on Biomedical Engineering*, 41:743–757, 1994.
14. F. B. Sachse. *Computational Cardiology*. Springer, Berlin, 2004.
15. E.J. Vigmond, R. Weber dos Santos, A.J. Prassl, M. Deo, and G. Plank. Solvers for the cardiac bidomain equations. *Progress in Biophysics and Molecular Biology*, 96(1-3):3–18, 2008.
16. N. Trayanova. Defibrillation of the heart: insights into mechanisms from modelling studies. *Experimental Physiology*, 91: 323–337, 2006.